Dual Function of Benzotriazole as Copper Alloy Corrosion Inhibitor and Hydrochloric Acid Flow Improver

Anees A. Khadom

Chemical Engineering Department, College of Engineering, Diyala University, Baquba City 32001, Diyala governorate, Iraq, e-mail: aneesdr@gmail.com

The corrosion of copper – nickel alloy in hydrochloric acid has been investigated at different temperatures, benzotrizole concentrations and corrosive solution velocities. Weight loss technique has been used to evaluate the corrosion rate data. Results obtained have proved that benzotrizole has a dual effect by reducing both metal corrosion and flow losses. Maximum inhibition efficiency was 91.5%, while maximum drag reduction was 52.4%. Several mathematical equations are suggested successfully to represent the data with high correlation coefficients. Molecular dynamic simulations have been also performed to investigate the adsorption behavior of the inhibitor on the copper alloy surface. One of the novelties of the given work is the analogy between the corrosion process and fluid flow, as well as the investigation of the dual effect of benzotriazole on the corrosion process and the flow losses.

Keywords: fluid flow, weight loss, rotating disc electrode, acid corrosion, drag reduction.

УДК 620.197

INTRODUCTION

Industrial equipment is often exposed to acidic action during the removal of scales and deposits. One of such acids, hydrochloric acid, may cause corrosion problems after cleaning processes. Various attempts have been made to prevent or retard the destructive effect of corrosion on metals and alloys. Using inhibitors is one of the most practical methods for protecting metals against corrosion, especially in acidic media [1]. Among numerous inhibitors, N-heterocyclic compounds are considered to be the most effective corrosion inhibitors [2]. Up to now, various N-heterocyclic compounds are reported as good corrosion inhibitors for steel in acidic media, such as imidazoline derivatives [3], 1,2,3-triazole derivatives [4], benzotriazole [5]. Generally, N-heterocyclic compounds exert their inhibition by adsorption on the metal surface through *N* heteroatom, as well as those with triple or conjugated double bonds or aromatic rings in their molecular structures. Furthermore, the adsorption of inhibitor on metal/solution interface is influenced by the chemical structure of inhibitor, the nature and charged surface of metal, the distribution of charge over the whole inhibitor molecule and the type of aggressive media [6]. Corrosion is a very important problem but not the only one. Another problem accompanying industrial flow system is friction losses. Therefore, the aim of present paper was to study the effect of temperature and velocity on the corrosion of copper – nickel alloy in hydrochloric acid in the presence of benzotrizole as a corrosion inhibitor and flow improver

EXPERIMENTAL WORK

The corrosion behavior of copper-nickel alloys, widely used in many industrial applications, was studied using weight loss in the absence and presence of benzotriazole (BTA) in 5% HCl solution at different temperatures (35, 45, 55 and 65^{o}C), different velocities (100, 200 and 300 rpm) and different inhibitor concentrations (0.001, 0.01 and 0.1M). Ring shape specimens of the Cu-Ni alloy were with the following dimensions: outside diameter 2.22 cm, width 1.5 cm, and thickness 0.13 cm, exposing a surface area of about 10 cm^2 to corrosive media. These specimens were fixed on a rotating shaft. Angular velocity was generated using *Tecquiment Limited Nottingham, UK*, system rotation with a range of 0-3000 rpm. The experimental work was done as mensioend in our privuos work [7]. Specimens were washed by a detergent and flushed by tap water followed by distilled water, degreased by analar benzene and acetone, then annealed in vacuum up to 600^{o}C for one hour and cooled under vacuum to room temperature. Before each run, specimens of Cu-Ni were abraded in sequence using emery paper of grade numbers 220, 320, 400, and 600, then washed by running tap water followed by distilled water, then dried by clean tissue, degreased with benzene, dried, degreased with acetone, dried, and finally left in desicater over silica gel. Weighing the specimen was carried out using 4 decimals digital balance and its dimensions were measured with vernier. The metal samples for weight loss runs were completely immersed in 250-cm^3 solution of corrodant contained in a conical flask. They were exposed for a period of three days at a desired temperature, acid concentration, and inhibitor concentration. Weight losses were determined in absence and presence of the inhibitor. The data are expressed as mass loss per unit time per unit area. In the given work the unit of the corrosion rate was the mass loss: g/m^2·day (gmd). The chemical composition of the Cu-Ni alloy was 0.148%Sn, 0.2%Fe, 0.134%Zn,

Table 1. Effect of velocity, inhibitor concentration and temperature on corrosion of Cu-Ni in 5% HCl solution in absence of inhibitor

No	Inhibitor concentration (M)	Temperature (^oC)	Velocity (rpm)	Corrosion Rate (gmd)	%*IE*
1	Nil	35	100	75.503	–
2			200	93.61	–
3			300	98.23	–
4		45	100	90.98	–
5			200	188.73	–
6			300	222.35	–
7		55	100	199.54	–
8			200	250.11	–
9			300	310.91	–
10		65	100	249.31	–
11			200	308.53	–
12			300	333.67	–
13	0.001	35	100	16.91	77.6
14			200	27.71	70.4
15			300	36.05	63.3
16		45	100	25.56	71.9
17			200	70.58	62.6
18			300	98.95	55.5
19		55	100	78.42	60.7
20			200	119.31	52.3
21			300	173.79	44.1
22			100	106.95	57.1
23		65	200	169.07	45.2
24			300	228.89	31.4
25	0.01	35	100	11.09	85.3
26			200	18.81	79.9
27			300	26.81	72.7
28		45	100	19.83	78.2
29			200	49.82	73.6
30			300	66.92	69.9
31		55	100	56.27	71.8
32			200	89.29	64.3
33			300	125.91	59.5
34		65	100	84.02	66.3
35			200	140.69	54.4
36			300	173.17	48.1
37	0.1	35	100	6.41	91.5
38			200	13.66	85.4
39			300	19.44	80.2
40		45	100	11.55	87.3
41			200	34.53	81.7
42			300	54.25	75.6
43		55	100	38.31	80.8
44			200	61.27	75.5
45			300	92.96	70.1
46			100	61.58	75.3
47		65	200	108.61	64.8
48			300	162.83	51.2

0.015%Al, 0.0003%P, 0.5%Sb, 0.0583%Pb, 0.0202%Si, 0.017%S, 0.0056%As, 10%Ni, and the remainder is Cu.

RESULTS AND DISCUSSIONS

Corrosion rate data

Table 1 shows the corrosion rate data of the Cu – Ni alloy in 5% HCl acid obtained at different temperatures and acid solution velocities in the absence and presence of BTA, a corrosion inhibitor, in different concentrations. Corrosion rates were obtained by the following equation [8]:

$$CR = \frac{\text{weight loss (g)}}{\text{area (m}^2\text{)}\times\text{time (day)}}. \quad (1)$$

From the corrosion rate, the percentage inhibition efficiency was calculated using the following equation:

$$IE\% = \frac{CR_{\text{uninibit}} - CR_{\text{inhibit}}}{CR_{\text{uninhibit}}} \times 100 \quad (2)$$

where $CR_{uninhibit}$ and $CR_{inhibit}$ are the corrosion rates in the absence and presence of the inhibitor, respectively. It is clear from Table 1 that the corrosion rate increased with both temperature and acid solution velocity, while it decreased with the inhibitor concentration. The data reveal that the inhibition efficiency of BTA enhances with increasing its concentration in the solution. The increase in the inhibition efficiency observed at a higher inhibitor concentration indicating that more inhibitors are adsorbed onto the metal surface, thus providing wider surface coverage. The maximum inhibitor efficiency was 91.5% at 0.1M inhibitor concentration, 100 rpm velocity and 35°C. The minimum value was 31.4% at 0.001M inhibitor concentration, 300 rpm acid solution velocity and 65°C.

Effect of inhibitor concentration and adsorption studies

It is generally accepted that organic molecules inhibit corrosion by adsorption on the metal/solution interface and that the basic information on the interaction between the inhibitor and the Cu – Ni alloy surface can be provided by the adsorption isotherm [9]. Surface coverage ($\theta = \%IE/100$) is often employed to character inhibitor adsorption. Many endeavors were made to fit these θ values to various isotherms and the best fit was found with the Langmuir adsorption isotherms (Fig. 1) [10]:

$$\frac{C}{\theta} = \frac{1}{K_{ads}} + C. \qquad (3)$$

Where C is the concentration of inhibitor, K_{ads} is the adsorptive equilibrium constant representing the interaction of additives with the metal surface, and θ is the surface coverage. The obtained parameters, such as linear regression coefficient (R^2) and K_{ads}, are listed in Table 2. The results show that all the linear regression coefficients and all the slopes are close to unity, which further confirms that the adsorption of BTA in 5% HCl follows the Langmuir adsorption isotherm. It is well known that K_{ads} depicts the interaction power between an adsorbate and an adsorbent. As seen from Table 2, the value of K_{ads} decreased with the increase in temperature and acid solution velocity, suggesting that more efficient adsorption was obtained at a lower temperature and velocity. So the inhibition efficiency decreased with the increase in temperature and acid motion as the result of the weakening of adsorption of BTA on the Cu – Ni surface. The values of the standard free energy of adsorption were obtained from the following equation [11]:

$$\Delta G^0_{ads} = -RT\ln(55.55\,K_{ads}) \qquad (4)$$

where R is the gas constant, T is the absolute temperature and the value of 55.55 is the molar concentration of water in solution expressed in M. According to the Van't Hoff equation [12]:

$$\ln K_{ads} = -\frac{\Delta H^0_{ads}}{RT} + \text{constant}. \qquad (5)$$

Thus, the adsorption enthalpy ΔH^0_{ads} was obtained by the linear regression between ln K_{ads} and $1/T$ (Fig. 2). In the experimental temperature range, the values of the adsorption enthalpy and adsorption entropy of the inhibition process could be approximately regarded as the standard adsorption enthalpy and adsorption entropy. Likewise, the standard adsorption entropy ΔS^0_{ads} could be calculated from the thermodynamic basic equation:

$$\Delta G^0_{ads} = \Delta H^0_{ads} - T\Delta S^0_{ads}. \qquad (6)$$

All the obtained thermodynamic parameters are listed in Table 2. The negative value of ΔH^0_{ads} also shows that the adsorption of the inhibitor is an exothermic process [13], indicating that the adsorption is strengthened with the decrease of temperature. The values of ΔS^0_{ads} agree with the result of other researchers [14, 15]. It is a well-known fact that adsorption is an exothermic phenomenon ($\Delta H^0_{ads} < 0$) accompanied by a decrease in entropy ΔS^0_{ads} [16]. Commonly, the adsorption type was regarded as physisorption whose inhibition action due to the electrostatic interactions between the charged molecules and the charged metal surface when the values of ΔG^0_{ads} reached up to -20 kJ·mol^{-1}, while the values around -40 kJ·mol^{-1} or smaller, were seen as chemisorption, which is due to the charges sharing or a transfer from the inhibitor molecules to the metal surface to form a covalent bond [17]. The value of ΔG^0_{ads} in the given work is around -29 kJ·mol^{-1}; suggesting that the adsorption of the inhibitor involves two types of interaction: chemisorption and physisorption.

Effect of temperature and kinetic parameters studies

Kinetic model was employed to further explain the inhibition properties of the inhibitor. The apparent activation energy for the corrosion process is calculated from the Arrhenius equation [18, 19]:

$$\ln CR = \ln A - \frac{E_a}{RT} \qquad (7)$$

where E_a is the apparent activation energy, A is the pre-exponential factor, T is the absolute temperature, R is the gas constant and CR is the corrosion rate. The Arrhenius plots of ln CR vs $1/T$ for the blank and various concentrations of BTA at the temperatures studied and 100 rpm are shown in Fig. 3. Similar figures were also obtained for other conditions. The values of E_a and A were calculated from the

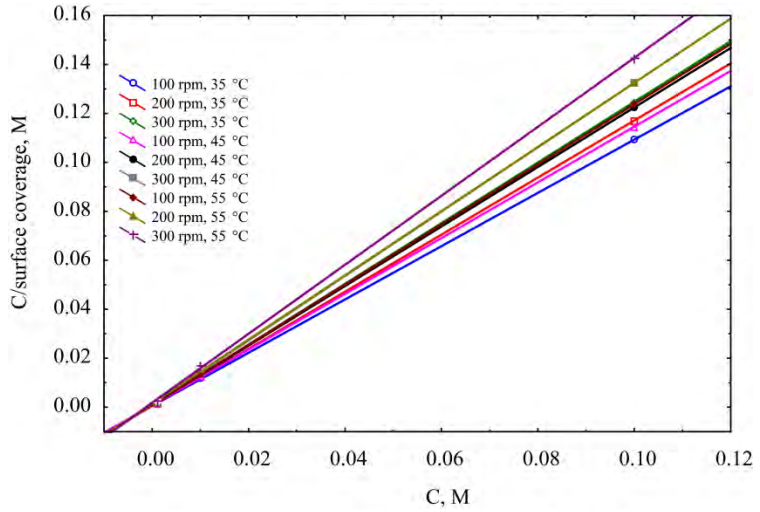

Fig. 1. Langmuir adsorption isotherms of BTA on Cu – Ni alloy surface at different conditions.

Table 2. Adsorption parameters of BTA on Cu – Ni alloy surface at different conditions

T (°C)	V (rpm)	R^2	Slope	K_{ads} (M^{-1})	ΔG^0_{ads} (kJ·mol^{-1})	ΔH^0_{ads} (kJ·mol^{-1})	ΔS^0_{ads} (kJ·K^{-1}·mol^{-1})
35	100	0.9998	1.088	2000	-29.75	- 37.58	-0.218
	200	0.9988	1.166	2000	-29.75		-0.218
	300	0.9978	1.239	1250	-28.54		-0.214
45	100	0.9969	1.138	1350	-29.67	- 36.83	-0.209
	200	0.9988	1.216	1250	-29.47		-0.208
	300	0.9999	1.315	1111	-29.16		-0.207
55	100	0.9998	1.228	1000	-29.79	- 34.27	-0.195
	200	0.9998	1.311	666	-28.68		-0.191
	300	0.9999	1.409	555	-28.18		-0.190
65	100	0.9998	1.327	998	-28.66	-32.33	-0.181
	200	0.9998	1.112	458	-26.69		-0.178
	300	0.9988	1.301	297	-24.22		-0.172

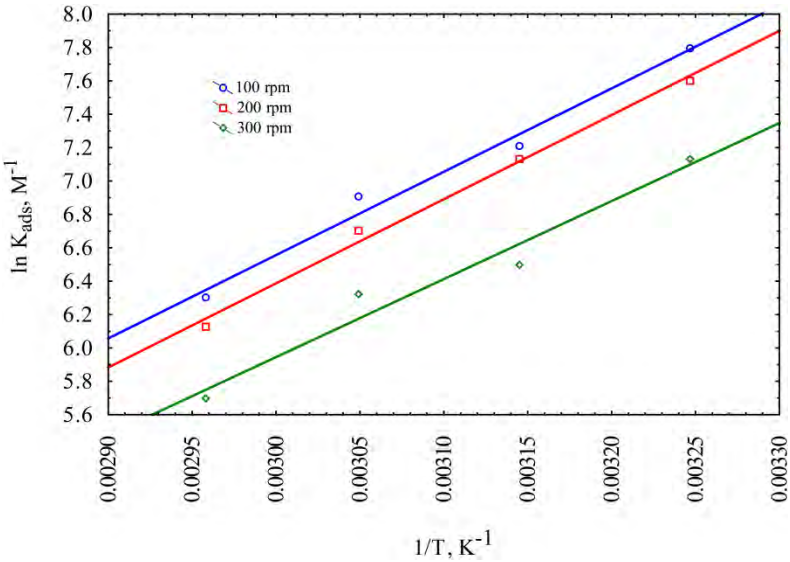

Fig. 2. Van't Hoff plot for the Cu – Ni/BTA/5%HCl system at different conditions.

slopes and intercepts of the Arrhenius plots, respectively. All the parameters are given in Table 3. All the linear regression coefficients (R^2) are close to unity, indicating that the Cu – Ni corrosion in 5% HCl can be elucidated using the kinetic model. According to Eq. (7), the corrosion rate of the Cu – Ni alloy depends on E_a and A. As seen from Table 3, the value of A in the presence of BTA is higher than that of the blank, so a lower corrosion rate of the Cu – Ni alloy is mostly lies on the higher apparent activation energy. A higher value of E_a was reported as physical adsorption that occurred in the first stage [20, 21]. The adsorption mode involves the change of the activation energy of the corrosion process with the addition of an inhibitor. According to Popova et al. [22], assuming that the electrochemical

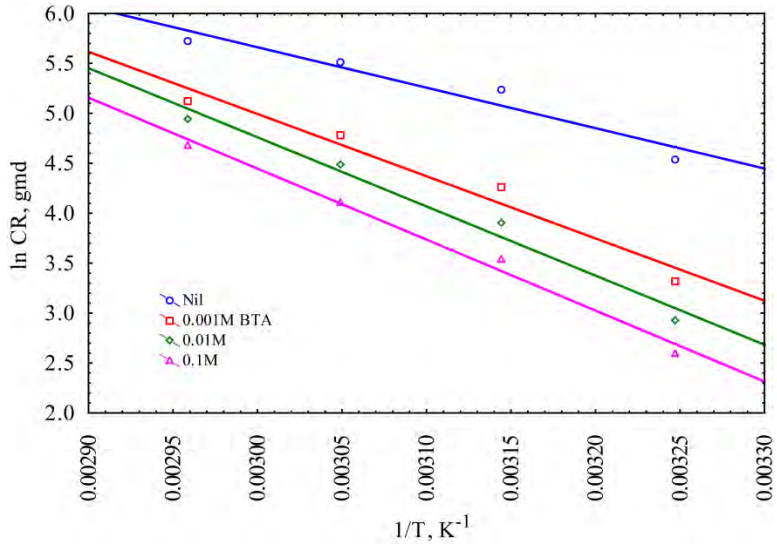

Fig. 3. Arrhenius plots for Cu – Ni alloy in 5% inhibited HCl acid at 200 rpm.

Table 3. Kinetics parameters of Arrhenius equation and transition state equation

C (M)	*V* (rpm)	Arrhenius equation			Transition state equation		
		R^2	*A* (gmd)	E_a (kJ·mol^{-1})	R^2	ΔH_a (kJ·mol^{-1})	ΔS_a (J·K^{-1}·mol^{-1})
Nil	100	0.9101	5.8×10^{08}	41.55	0.9149	38.22	-86.64
0.001		0.9345	2.3×10^{12}	66.31	0.9221	61.55	-22.68
0.01		0.9777	3.9×10^{12}	68.35	0.9689	65.43	-13.33
0.1		0.9615	7.5×10^{12}	73.57	0.9639	70.55	-5.84
Nil	200	0.9948	3.4×10^{06}	28.22	0.9478	25.75	-80.99
0.001		0.9791	9.9×10^{11}	61.42	0.9817	59.11	-21.84
0.01		0.9832	3.7×10^{12}	66.68	0.9888	63.13	-11.83
0.1		0.9811	4.9×10^{12}	70.83	0.9887	67.11	-11.17
Nil	300	0.9633	6.2×10^{05}	25.35	0.9947	22.62	-78.01
0.001		0.9621	6.9×10^{10}	59.56	0.9856	57.45	-19.49
0.01		0.9878	4.1×10^{11}	63.65	0.9268	61.56	-8.15
0.1		0.9841	2.8×10^{12}	66.66	0.9248	65.07	-11.17

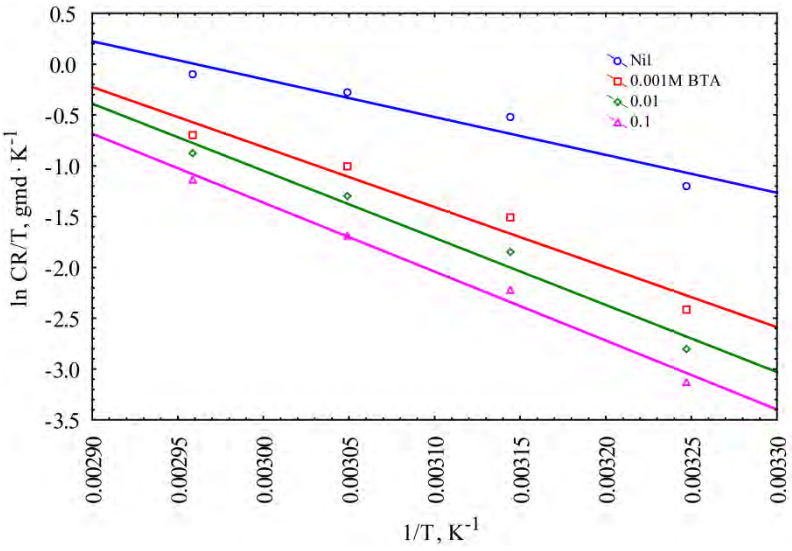

Fig. 4. Transition state plots for Cu – Ni alloy in 5% inhibited HCl acid at 200 rpm.

corrosion is a heterogeneous reaction, the pre-exponential factor in the Arrhenius equation *A* is related to the number of active centers. There are two possibilities related to these active centers with different E_a on the metal surface: In the first case, the activation energy in the presence of inhibitor molecules is lower than that of pure acidic media ($E_{a,inh} < E_{a,HCl}$), a smaller number of more active sites remain uncovered, which takes part in the corrosion process [22]. In the other case, ($E_{a,inh} > E_{a,HCl,}$) an inhibitor is adsorbed on the most active adsorption sites (having the lowest energy) and the corrosion process takes place chiefly on the active sites (having higher energy). In the experiment for the

given study, the values of A and E_a in the presence of inhibitor molecules are higher than those in a pure hydrochloric acid, which are consistent with the latter mentioned above. This means that the adsorbed BTA molecules block the most active sites, while the sites of a higher activation energy, which are greater in number, take part in the subsequent corrosion [21]. An alternative formulation of the Arrhenius equation is the transition state equation [23]:

$$CR = \frac{RT}{Nh}\exp\left(\frac{\Delta S_a}{R}\right)\exp\left(-\frac{\Delta H_a}{RT}\right) \quad (8)$$

where h is Plank's constant and N is Avogadro's number. The values of the entropy of activation ΔS_a and of the enthalpy of activation ΔH_a were obtained by drawing of information from equation 8 as ln (CR/T) vs ($1/T$) as shown in Fig. 4. These values were also listed in Table 3. The behavior of ΔH_a values was similar to E_a. As observed, for all cases $E_{act} > \Delta H_{act}$ by a value approximately equal to RT. From the thermodynamic and kinetic points of view, the unimolecular reactions are characterized by the following equation [24]:

$$E_a - \Delta H_a = RT. \quad (9)$$

The negative values of ΔS_a pointed to a greater order produced during the process of activation. This can be achieved by the formation of an activated complex that represents association or fixation with a consequent loss in the degree of freedom of the system during the process [25].

Effect of velocity and fluid flow studies

Table 1 shows that under various conditions, as the velocity increased, the corrosion rate also increased. The effect of flow on the corrosion rate of copper has been used in a number of instances to determine whether corrosion is under activation, diffusion, or mixed control. It was demonstrated that the linear increasing of the corrosion rate with velocity indicates that the corrosion proceeds under diffusion control, while its slightly increase indicate the mixed control process and no effect of velocity on the activation control process. Figure 5 shows the effect of velocity on the corrosion rate in the absence of an inhibitor, which suggests the mixed control corrosion process. The higher the temperature, the stronger the effect of the speed of rotation on the corrosion process. A similar behavior was observed in the presence of inhibitor. The enhancement of the fluid flow generally results in the metal total weight loss by supplying the corrosives at faster rates. Relative metal/environment motion thins the quiescent layers at the metal leading to less restriction of corrosives by diffusion process. When velocity becomes extremely high mechanical effects add to corrosion and increase the damage to metals (i.e. erosion). One of the important things of present work is the analogy between corrosion process and fluid flow, and to explore the dual effect of BTA as corrosion inhibitor and flow improve material. Table 4 shows the physical properties of the corrosive solution in the presence and absence of BTA at different conditions, the Reynolds numbers, and Funning friction factor. The Reynolds number can be defined as follows:

$$\mathrm{Re} = \frac{\rho\, u\, d}{\mu} \quad (10)$$

where ρ is the solution density (kg·m^{-3}), u is the linear velocity (m·s^{-1}), d is the sample diameter (m), and μ is the dynamic solution viscosity (Pa·s). Blasius' equation can be used to evaluate the values of the Fanning factor as:

$$f = 0.0791\, R^{-0.25}. \quad (11)$$

Equation 11 is valid for turbulent flow and smooth pipes [26]. The rotating working cylinder electrode was assumed to be the pipe, and the angular velocity was converted to linear velocity. Flow improvement can be measured using the equation of drag reduction [27]:

$$\%Dr = \frac{\Delta P_b - \Delta P_a}{\Delta P_b} \times 100\% \quad (12)$$

where $\%Dr$ is percentage of the drag reduction, ΔP_b and ΔP_a is the pressure drop before and after addition of BTA. Pressure drop as a function of the Fanning friction factor can be written in the form [26]:

$$\Delta P = 4\, f\, (\frac{L}{d})\, \frac{\rho\, u^2}{2} \quad (13)$$

where L is the cylinder length (m). Substituting Eq. 13 in Eq. 12 and eliminating the constants from denominator and numerator, the following equation can be obtained:

$$\%Dr = \frac{f_{un} - f_{in}}{f_{un}} \times 100\% \quad (14)$$

where f_{un} and f_{in} are the Fanning friction factors of uninhibited and inhibited 5% HCl solutions. Table 4 and Fig. 6 show that the values of $\%Dr$ increased with a higher inhibitor concentration. This behavior is attributed to the formation of an inhibition layer that may reduce the friction between metal and solution. However, the inhibition efficiency of BTA was greater than its drug reduction. As noticed above, many variables can affected the values of the drag reduction. Therefore, the dimensional analysis was used in the given work for grouping the significant quantities into a dimensionless group in order to reduce the number of variables appearing and to make the result compact and applicable to all similar situa-

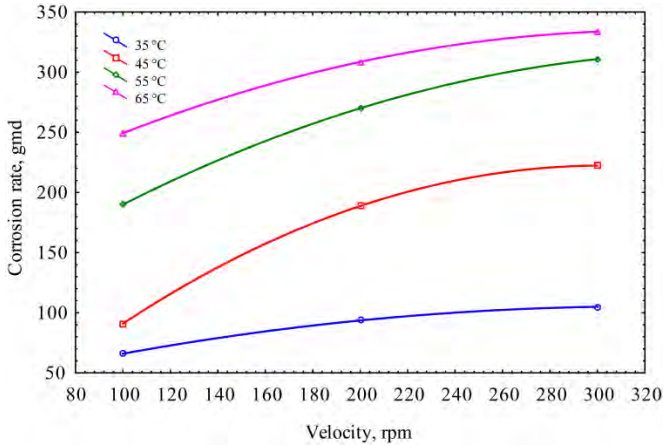

Fig. 5. The effect of velocity on the corrosion of Cu-Ni Alloy in 5% HCl solution in absence of inhibitor.

Table 4. Physical properties of 5% inhibited HCl solution at different operating conditions, Reynolds numbers, and friction factors

BTA	Temperature, °C	Density, kg·m^{-3}	Viscosity, Pa·s × 10^{-4}	Velocity (rpm)	Re × 10^3	f × 10^{-4}	%*Dr*
Nil	35	1018.01	6.94	100	3.77	100.84	0
	45	1014.10	5.85		4.46	96.73	0
	55	1009.60	5.01		5.20	93.12	0
0.001M	35	9999.51	6.89		37.36	56.81	43.66
	45	9999.43	5.85		44.09	54.58	43.57
	55	9999.26	5.01		51.53	52.49	43.63
0.01M	35	9999.42	6.50		39.63	56.05	44.41
	45	9999.33	5.51		46.83	53.76	44.47
	55	9999.20	4.71		54.77	51.71	44.46
0.1M	35	9998.61	3.62		71.52	48.36	52.04
	45	9998.55	3.01		85.64	46.23	52.21
	55	9998.43	2.54		101.45	44.32	52.42
Nil	35	1018.01	6.94	200	7.56	84.83	0
	45	1014.10	5.85		8.94	81.33	0
	55	1009.60	5.01		10.41	78.31	0
0.001M	35	9999.51	6.89		74.82	47.82	43.62
	45	9999.43	5.85		88.30	45.88	43.58
	55	9999.26	5.00		103.20	44.13	43.64
0.01M	35	9999.42	6.50		79.37	47.12	44.45
	45	9999.33	5.51		93.78	45.21	44.41
	55	9999.20	4.71		109.69	43.46	44.51
0.1M	35	9998.61	3.60		143.23	40.66	52.06
	45	9998.55	3.01		171.51	38.86	52.21
	55	9998.43	2.54		203.17	37.25	52.43
Nil	35	1018.01	6.94	300	11.33	76.66	0
	45	1014.10	5.85		13.39	73.52	0
	55	1009.60	5.01		15.59	70.78	0
0.001M	35	9999.51	6.89		112.02	43.23	43.61
	45	9999.43	5.84		132.21	41.48	43.57
	55	9999.26	5.01		154.51	39.89	43.64
0.01M	35	9999.42	6.51		118.84	42.61	44.41
	45	9999.33	5.51		140.42	40.86	44.42
	55	9999.20	4.71		164.23	39.29	44.49
0.1M	35	9998.61	3.60		214.45	36.75	52.06
	45	9998.55	3.01		256.79	35.13	52.21
	55	9998.43	2.54		304.21	33.68	52.41

tions. The drag reduction is influenced by the physical properties of the solvent and properties of the flow. The relationship may be written as:

$$\Delta P = f(d, \mu, \rho, V, C, L, \varepsilon, T). \quad (15)$$

By applying the dimensional analysis, the following non-dimensional relation was proposed:

$$\%Dr = f(\mathrm{Re}, \varepsilon/d, L/d, C, T) \quad (16)$$

or

$$\%Dr = a(\mathrm{Re})^b \left(\frac{\varepsilon}{d}\right)^c \left(\frac{L}{d}\right)^d (C)^k (T)^h \quad (17)$$

where *a*, *b*, *c*, *d*, *k* and *h* are constants, and ε is the roughness of metal. There are many assumptions and facts to be taken into account:

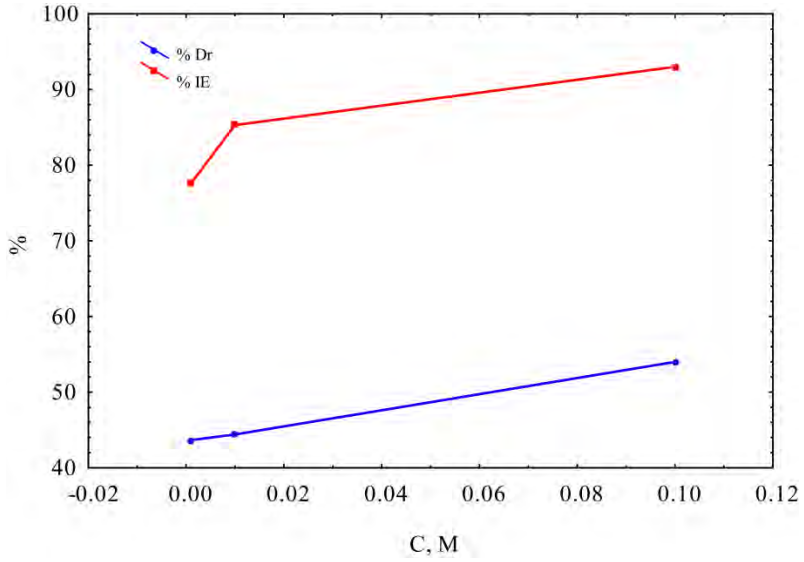

Fig. 6. Behavior of %*IE* and %*Dr* with inhibitor concentration at 35°C and 100 rpm.

1. The working electrode is smooth, i.e. roughness term is neglected.

2. The ratio *L*/*d* is constant.

3. From Table 4, the effect of temperature on %*Dr* is insignificant.

Then, Eq. 17 can be reduced to the following one:

$$\%Dr = a\,\mathrm{Re}^{b}\,C^{k}. \tag{18}$$

The method of least squares was used to determine the coefficients of correlation for the Reynolds number range (3779.11 – 304205.85), which yields the following equation with 0.9236 correlation coefficient.

$$\%Dr = 45.12\,\mathrm{Re}^{0.02}\,C^{0.04}. \tag{19}$$

Mathematical and statistical studies

Statistical analysis can be used to determine the effects of each variable on the corrosion rate of the Cu – Ni alloy. One of these analyses is a nonlinear regression of the data of Table 1. A third-order fitting equation can be used to know whether the variables affect Cu – Ni individually or there is an interaction effect. Most of probabilities can be taken into account, the main effect of each variable and the interaction effect:

$$\begin{aligned} CR = {} & b_0 + b_1T + b_2C + b_3V + b_4TC + \\ & + b_5TV + b_6CV + b_7T\,CV + b_8T^2 + \\ & + b_9C^2 + b_{10}V^2 + b_{11}T^3 + b_{12}C^3 + b_{13}V^3 \end{aligned} \tag{20}$$

where b_0 is constant, b_1, b_2, b_3 are linear coefficients, b_4, b_5, b_6, b_7 are interaction coefficients, b_8, b_9, b_{10} are quadratic coefficients and b_{11}, b_{12}, b_{13} are cubic coefficients. The above model can be estimated using the Levenberg-Marquardt method, and the following equation can be obtained with 0.9795 correlation coefficient:

$$\begin{aligned} CR = {} & 8150092 - 1309T - \\ & - 1.1\times10^{5}C + 1.4\times10^{5}V - \\ & - 26TC + 0.012TV - 5.4CV - \\ & - 0.043TCV + 4.1T^2 + 1.1\times10^{7}C^2 + \\ & + 810.3V^2 - 1289\times10^{-6}T^3 + \\ & + 9.5\times10^{-7}C^3 + 19\times10^{-6}V^3. \end{aligned} \tag{21}$$

The analysis of variance (F-test) was used to test the significance of each effect in equation 21 [28]. The calculations are given in Table 5. An estimate of the variance S_b^2 is obtained by dividing the experimental error variance S_r^2 by the sum of squares of each effect ΣX^2, as follows: $S_b^2 = \frac{S_r^2}{\sum X^2}$ where, $S_r^2 = \frac{\sum e^2}{\gamma}$ and $\gamma = N–n$ is the degree of freedom. The significance of effects may be estimated by comparing the values of the ratio (b^2/S_b^2) with the critical value of the F-distribution at 95% confidence level ($F_{0.95} = 6.61$). If $b^2/S_b^2 > 6.61$, then the effect is significant. Thus, according to the results shown in Table 5, it appears that the cubic and most of quadratic effects are insignificant, while the interaction effects and the main effect of each variable are the dominated ones. The best response function is then conveniently written as follows:

$$\begin{aligned} CR = {} & 8150092 - 1309T - 1.1\times10^{5}C + \\ & + 1.4\times10^{5}V - 26TC + 0.012TV - 5.4CV - \\ & - 0.043TCV + 4.1T^2. \end{aligned} \tag{22}$$

Another equation can be suggested to represent the corrosion rate data. This model depends on the discussion mentioned above. Instead of using multi-terms model (eq. 21), a one-term model can be used. A similar model was suggested successfully in our previous studies [29, 30]. It was found out that the Cu – Ni alloy corrosion varies exponentially with

Table 5. Analysis of variance

Effect	ΣX^2	Coefficients, b (units)		Variance $S_b^2 = \frac{S_r^2}{\sum X^2}$	F-value $= b^2 / S_b^2$	$F_{0.95}$ = 6.61
		b_0 (gmd)	815×10^4			
T	75300	b_1 (gmd·K^{-1})	-1309	0.763	224×10^4	*S**
C	0.091	b_2 (gmd·M^{-1})	-11×10^3	1.77×10^{-26}	203×10^{12}	*S*
V	168×10^4	b_3(gmd·rpm^{-1})	14×10^4	9212.4	212×10^4	*S*
TC	190.15	b_4 (gmd·M^{-1}K^{-1})	-26	0.043	157×10^2	*S*
TV	35×10^8	b_5 (gmd·rpm^{-1}K^{-1})	0.012	1.33×10^{-16}	107×10^{10}	*S*
CV	4242.42	b_6 (gmd·M^{-1}rpm^{-1})	5.4	0.0041	6985.35	*S*
TCV	887×10^4	b_7 (gmd·rpm^{-1}M^{-1}K^{-1})	-0.043	2×10^{-11}	96×10^6	*S*
T^2	177×10^6	b_8 (gmd·K^{-2})	4.1	3×10^{-9}	5.3×10^9	*S*
C^2	9×10^{-4}	b_9 (gmd·M^{-2})	11×10^6	33×10^{12}	3.559	*NS*
V^2	11×10^{10}	b_{10} (gmd·rpm^{-2})	810.3	39×10^6	3.05	*NS*
T^3	34×10^{16}	b_{11} (gmd·K^{-3})	13×10^{-6}	4×10^7	3.11	*NS*
C^3	9×10^{10}	b_{12} (gmd·M^{-3})	95×10^{-7}	2.8×10^{21}	3.2×10^{-34}	*NS*
V^3	72×10^{24}	b_{13} (gmd·rpm^{-3})	19×10^{-6}	39×10^{12}	4.56	*NS*
* *S*: significant effect, *NS*: not significant effect						

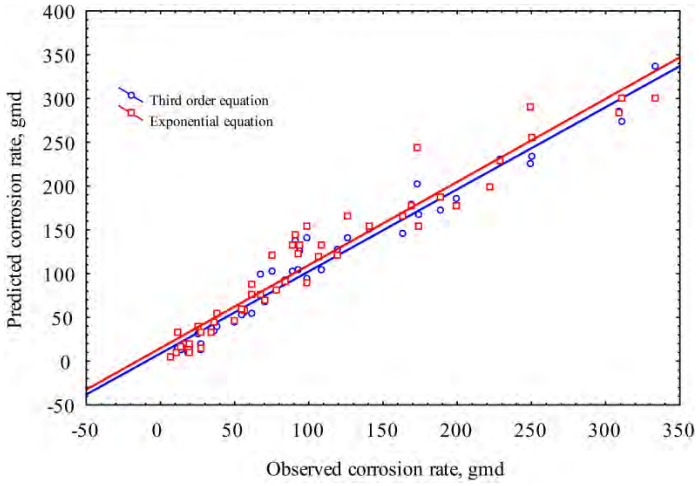

Fig. 7. Predicted corrosion rate against observed one.

the absolute value of temperature (according to the Arrhenius eq.), in the same way it is proportional to the speed of rotation and BTA concentration as follows:

$$CR \propto \exp(\frac{1}{temp.})(\frac{1}{C})(V) \quad (23)$$

Re-arranging equation 23 we get:

$$CR = b_{14} C^{-b_{15}} V^{b_{16}} \exp(\frac{b_{17}}{T}) \quad (24)$$

where b_{14}, b_{15}, b_{16}, b_{17} are other coefficients and T is the absolute temperature (*K*). This equation can be estimated using the above-mentioned estimation method producing the following equation with 0.9773, correlation coefficient:

$$CR = 5.6\times10^7 C^{-0.066} V^{0.576} \exp(\frac{-5476}{T}). \quad (25)$$

Generally, correlation coefficient up to 0.30 indicates a weak relationship and is of uncertain validity that between 0.50 and 0.70 indicates a significant relationship and is of practical importance, while the one above 0.90 means a strong relationship [30]. Figure 7 shows the predicted corrosion rates by a third-order polynomial model and an exponential model against experimental values. Eq. 25 is easier and more practical than Eq. 22 since it deals with only one term. The coefficient b_{17} in Eq. 25 can be compared with the slope of the Arrhenius equation (-*E*/*R*). The activation energy value by Eq. 25 equals to 45.53 kJ/mol, within the range of the activation energy given in Table 3. Also the value of coefficient b_{14} is comparable with the frequency factor values.

Theoretical and quantum chemical studies

Theoretical and quantum chemical calculations have been used to explain the mechanism of corrosion inhibition, [31, 32]. Quantum chemical calculations are proven to be a very powerful tool to understand the inhibition mechanism and to emphasize the experimental data [33, 34]. Through the method of quantum chemical calculations, structural parameters such as the frontier molecular orbital (MO), the highest occupied molecular orbital (HOMO), the

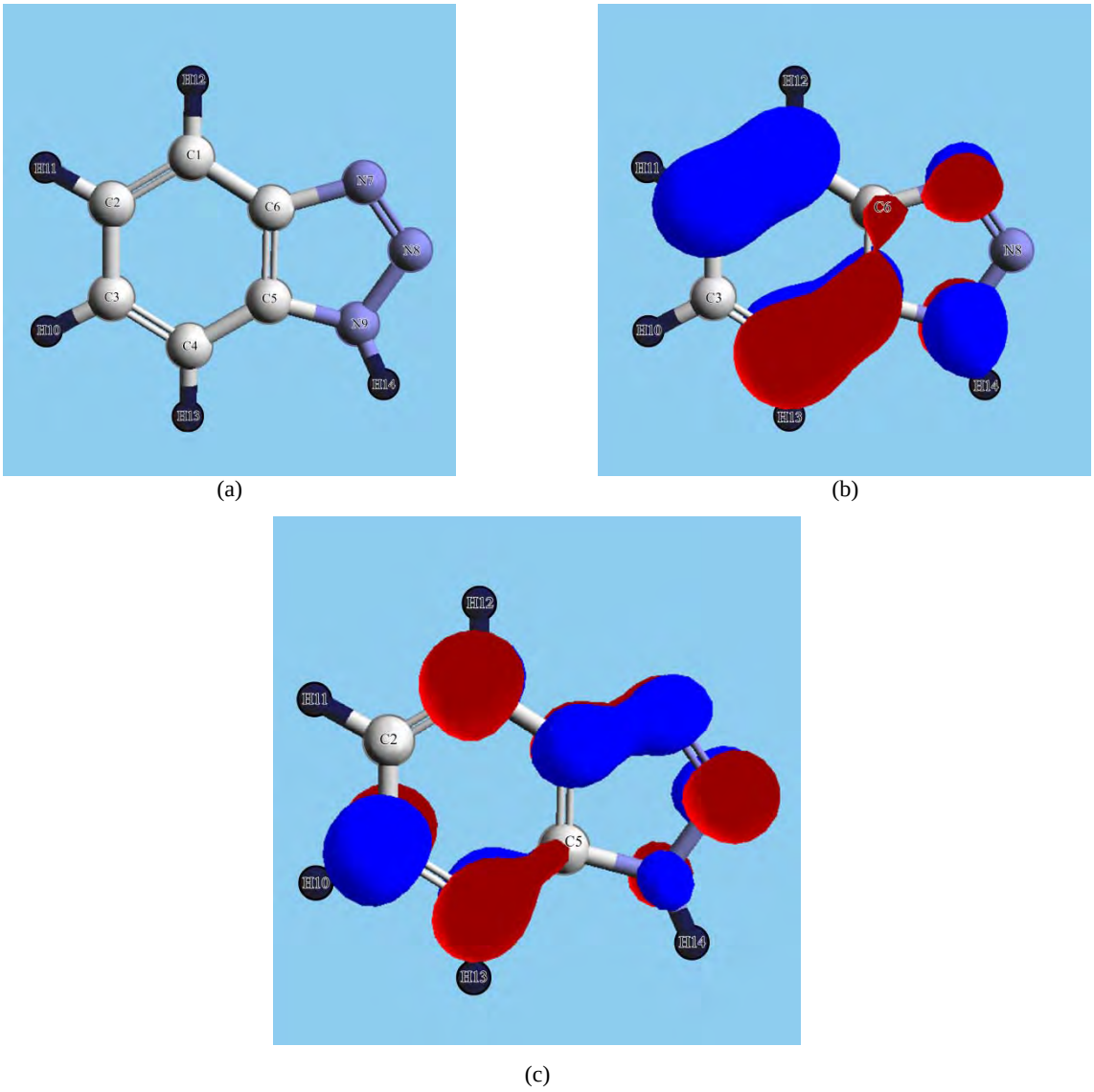

Fig. 8. (a) Optimized BTA structure; (b) HOMO distribution; (c) LUMO distribution.

lowest unoccupied molecular orbital (LUMO), dipole moment (μ) and the fraction of electrons (Δ*N*) transfer from inhibitors to the metal surface were calculated and correlated with corrosion inhibition efficiencies. The structure of the inhibitor was optimized by the ArgusLab 4.0.1 package. The quantum chemical parameters were estimated by the PM3-SCF method. The optimized minimum energy geometrical configurations of tested compounds are given in Fig. 8a. The computed quantum chemical parameters like the energy of the highest occupied molecular orbital (E_{HOMO}), the energy of the lowest unoccupied molecular orbital (E_{LUMO}), HOMO–LUMO energy gap and the dipole moment are summarized in Table 6. It has been well documented in literature [35] that the higher the value of E_{HOMO} of the inhibitor, the greater is the ease of the inhibitor to offer electrons to unoccupied *d* orbital of the metal atom, and the higher is the inhibition efficiency of the inhibitor. Furthermore, the lower the E_{LUMO}, the easier is the acceptance of electrons from the metal atom to form feedback bonds. The gap between HOMO–LUMO energy levels of molecules was another important parameter that needs to be considered. The smaller the value of Δ*E* of an inhibitor, the higher is the inhibition efficiency of that inhibitor [36]. Further higher values of dipole moment will favor the enhancement of corrosion inhibition [37]. The number of transferred electrons (Δ*N*) was also calculated according to Eq. 26 [37]

$$\Delta N = \frac{X_{Cu} - X_{inh}}{2(\eta_{Cu} - \eta_{inh})} \tag{26}$$

where X_{Cu} and X_{inh} denote the absolute electronegativity of iron and the inhibitor molecule, respectively; η_{Cu} and η_{inh} denote the absolute hardness of iron and the inhibitor molecule, respectively. These quantities are related to the electron affinity (*A*) and ionization potential (*I*)

$$X = \frac{I + A}{2}$$
$$\eta = \frac{I - A}{2} \tag{27}$$

Table 6. Quantum chemical parameters for BTA on Cu – Ni alloy

E_{HOMO} (eV)	E_{LUMO} (eV)	ΔE (eV)	Dipole moment, μ (debye)	ΔN
-9.438	-0.685	8.795	3.751	0.066

Table 7. Mulliken atomic charges for BTA

No	Atom	Charge	No	Atom	Charge
1	C	-0.0909	8	N	-0.0999
2	C	-0.2187	9	N	0.0916
3	C	-0.1517	10	H	0.1939
4	C	-0.1747	11	H	0.1996
5	C	-0.1763	12	H	0.2153
6	C	-0.1542	13	H	0.2079
7	N	-0.0092	14	H	0.1672

In turn, I and A are related to E_{HOMO} and E_{LUMO}:

$$I = -E_{HOMO}, \quad A = -E_{LUMO}. \tag{28}$$

Values of X and η were calculated by using the values of I and A obtained from the quantum chemical calculation. The theoretical values of X_{Cu} and η_{Cu} are 4.48 and 0 eV/mol, respectively [38]. The fraction of electrons transferred from the inhibitor to the iron molecule (ΔN) was calculated. According to other reports [39], the value of ΔN showed an inhibition effect as a result from electrons donation. According to Lukovits et al. [40], if $\Delta N < 3.6$, then the inhibition efficiency increases with increasing electron-donating ability at the metal surface. In this study, BTA was the donor of electrons, and the copper oxide surface was the acceptor. BTA was bound to the copper oxide surface and thus formed an inhibitive adsorption layer against corrosion. The Mulliken charge distributions of the inhibitors are presented in Table 7. It can be readily noticed that carbon and nitrogen atoms have higher charge densities. The regions of the highest electron density are generally the potential sites for the electrophiles attacked [40, 41]. The use of the Mulliken population analysis to probe the adsorption center of inhibitors has been reported earlier [42]. Based on Mulliken charge calculations, highest electron densities were located on N and C atoms implying that those atoms were active centers, which have the strongest ability of bonding to the Cu – Ni surface. On the other hand, HOMO (Fig. 8b) was mainly distributed on the area containing carbon and nitrogen atoms and this area is probably the primary site of the bonding. It was found out that those inhibitors apart from existing in the cationic form can also interact with the metal surface through the electrostatic attraction. This interaction with the metal surface with several numbers of active centers leads to the formation of a protective layer on the Cu – Ni alloy surface.

Corrosion and inhibition mechanism of Cu-Ni alloy

Anodic dissolution of copper in chloride media has been studied extensively [43–45]. The accepted anodic reaction of HCl solution is the dissolution of copper through oxidation of Cu (0) to Cu^+:

$$Cu \rightarrow Cu^+ + e. \tag{29}$$

Then Cu^+ reacts with chloride ion from the solution to form CuCl

$$Cu^+ + Cl^- \rightarrow CuCl. \tag{30}$$

Insoluble CuCl precipitates on the copper surface. The CuCl species has poor adhesion, is unable to produce enough protection for the copper surface, and transforms into the sparingly soluble cuprous chloride complex, $CuCl^{-2}$ [46];

$$CuCl + Cl^- \rightarrow CuCl_2^-. \tag{31}$$

It has also been reported that $CuCl_2$ adsorbed on the surface dissolves by further oxidation [45]

$$CuCl_{2\,ads}^- \rightarrow Cu^{2+} + 2Cl^- + e. \tag{32}$$

It is also stated that the anodic dissolution of copper in the acidic chloride solution is controlled by both electro dissolution of copper and diffusion of $CuCl^-_2$ to the solution bulk [45, 46]. These conclusions agree with the results of the given work. The cathodic corrosion reaction in an aerated acidic chloride solution is:

$$4H^+ + O_2 + 4e^- \rightarrow 2H_2O. \tag{33}$$

The total corrosion reaction of copper in acidic chloride solutions is then as follows:

$$2Cu + 4H^+ + 4Cl^- + O_2 \rightarrow \rightarrow 2Cu^{2+} + 4Cl^- + 2H_2O. \tag{34}$$

The inhibition mechanism depends on the effect of an inhibitor in the above equations. BTA is an organic compound consisting of benzene and triazole rings with a formula of $C_6H_5N_3$ which can exist in the following tautomeric forms [47]:

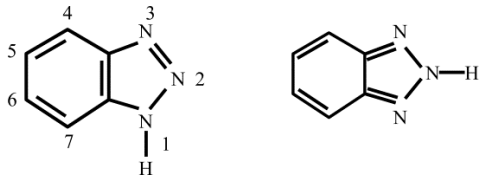

BTA can exist in a protonated form (BTAH), which can be presented as below:

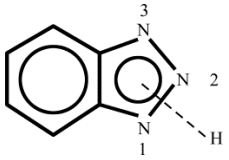

This last structure shows that BTAH can act as a weak acid by releasing a proton or a base by accepting a proton to one of the nitrogen lone pairs of

electrons. On the other hand, BTAH can utilize the lone pairs of electrons existing on nitrogen atoms to bond itself to the copper surface. In this way, a coordination compound can be formed on the copper alloy surface that can act as an inhibitor against corrosion. This makes benzotriazole one of the most efficient inhibitors for the corrosion of copper and its alloys in queous media [48, 49]. Generally, BTAH acts as an anodic or mixed-type corrosion inhibitor [50–52] via its physisorpion [53, 54] on the copper surface that follows, in most cases, the Langmuir isotherm [53, 54]. One of proposed mechanism attributed the inhibition efficiency of BTAH to the formation of a protective film of $Cu_{(I)}$ BTA complex on the metal surface, i.e.

$$Cu + [BTAH] \Leftrightarrow Cu_{(I)}[BTA] + H^+ + e^-. \quad (35)$$

There is an ample evidence that the $Cu_{(I)}$ BTA complex exists in a polymeric form which further stabilizes the film:

$$n(Cu_{(I)}(BTA)) \Leftrightarrow \left[Cu_{(I)}BTA\right]_n. \quad (36)$$

This polymeric chain has alternating copper atoms and BTAH molecules with the following proposed structure [55]

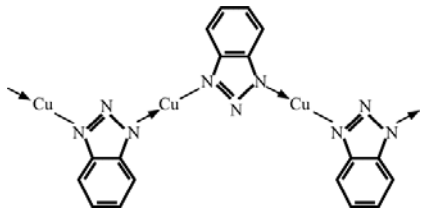

These were primarily concerned with the equilibrium properties of the protective film and its effects on the anodic and cathodic partial reactions. Youda et al. [56] have suggested that adsorption and complex formation are in equilibrium, i.e.

$$n\ BTAH_{ads} + n\,Cu \Leftrightarrow \left[Cu_{(I)}BTA\right]_n + n\ H^+ + n\,e^-. \quad (37)$$

Equation 37 reveals that by increasing the pH value, both the potential in the noble direction and the inhibitor concentration favor the formation of the protective polymeric complex, while adsorption becomes favorable in acidic media, at a lower inhibitor concentration and when the potential changes to more negative values, with the rate of adsorption of BTAH on a Cu_2O surface being faster than that on a CuO surface [47]. The inhibition efficiency of BTAH in a specific medium can be explained via its chemical properties. Based on the pH of the medium, BTAH can exist in either one of three forms [56]. In strongly acidic media, BTAH can exist in a protonated form $BTAH^+_2$, while in weakly acidic, neutral, and weakly alkaline media it has the form BTAH. On the other hand, in strongly alkaline media it is BTA^-. Considering that Cu surface is positively charged in the solution, it can easily be concluded which form is more and which is less favorable.

CONCLUSIONS

The main conclusions of the given study can be summarized as follows:

1. Measurements have demonstrated that under the chosen experimental conditions BTA offers sufficient protection against corrosion for the copper – nickel alloy in 5% HCl solutions.

2. BTA adsorbs on a metal surface and, according to the Langmuir adsorption isotherm, forms a protective monolayer.

3. Heat of adsorption values are within the range of physical and chemical adsorption.

4. Corrosion rate of the copper – nickel alloy increases with temperature, according to the Arrhenius equation, with a higher activation energy in the presence of BTA.

5. Corrosion rate of the copper – nickel alloy increases with the speed of rotation. The nonlinear increase of corrosion rate with velocity indicates that the reaction takes place according to both the mass transfer effect and the charge surface reaction.

6. Molecular dynamic simulations have been performed to investigate the adsorption behavior of BTA on the copper alloy surface.

7. This study has demonstrated that BTA has a dual effect in the Cu – Ni alloy/HCl/system. In addition to being a good corrosion inhibitor effect, it acts as a flow improver agent.

ACKNOWLEDGEMENTS

This work was supported by Baghdad University, College of Engineering, Chemical Engineering Department, which is gratefully acknowledged.

REFERENCES

1. Trabanelli G. Inhibitors an Old Remedy for a New Challenge. *Corrosion*. 1991, **47**(1), 410–419.

2. Bentiss F., Traisnel M., Gengembre L, Lagrenée M. Inhibition of Acidic Corrosion of Mild Steel by 3,5-diphenyl-4H-1,2,4-triazole. *Appl Surf Sci*. 2000, **161**(2) 194–202.

3. Cruz J., Martnez R., Genesca J., Garca-Ochoa E. Experimental and Theoretical Study of 1-(2-ethylamino)-2-methylimidazoline as an Inhibitor of Carbon Steel Corrosion in Acid Media. *J Electroanal Chem*. 2004, **566**(1), 111–121.

4. Abdennaby A.M., Abdulhady A.I., Abu-Oribi S.T., Saricimen H. The Inhibition Action of 1 (benzyl)1-H-4,5-dibenzoyl-1,2,3-triazole on Mild Steel in Hydrochloric Acid Media. *Corros Sci*. 1996, **38**(10), 1791–1800.

5. Gomma G.K. Corrosion Inhibition of Steel by Benzotriazole in Sulphuric Acid. *Materials Chemistry and Physics*. 1998, **55**(1) 235–240.

6. Khadom A.A. Effect of Corrosive Solution Motion on Copper – Nickel Alloy Pipe in Presence of

Naphthylamine as a Corrosion Inhibitor. *Journal of Materials and Environmental Science*, 2013, **4**(4), 510–519, 2013.

7. Khadom A.A., Aprael S. Yaro and Abdul Amir H. Kadhum**.** Adsorption Mechanism of Benzotriazole for Corrosion Inhibition of Copper-nickel Alloy in Hydrochloric Acid. *J Chil Chem. Soc*. 2010, **55**(1), 150–152.
8. Yaro A.S., Khadom A.A., Ibraheem H.F. Peach Juice as an Anti-corrosion Inhibitor of Mild Steel. *Anti–Corros Method M*. 2011, **58**(3), 116–124.
9. Singh A.K. Quraishi M.A. Effect of Cefazolin on the Corrosion of Mild Steel in HCl Solution. *Corros Sci*. 2010, **52**(1), 152–160.
10. Martinez S., Tagljar I. Correlation between the Molecular Structure and the Corrosion Inhibition Efficiency of Chestnut Tannin in Acidic Solutions. *J Mol Struc-THEOCHEM*. 2003, **640**(1), 167–174.
11. Cano E., Polo J.L., La Iglesia A., Bastidas J.M. A Study on the Adsorption of Benzotriazole on Copper in Hydrochloric Acid Using the Inflection Point of the Isotherm. *Adsorption*. 2004, **10**(3) 219–225.
12. Do D. D. *Adsorption Analysis: Equilibria and Kinetics*. London: Imperial College Press, 1980. 892 p.
13. Gomma M.K., Wahdan M.H. Schiff Bases as Corrosion Inhibitors for Aluminium in Hydrochloric Acid Solution. *Mat Chem Phys*. 1995, **39**(3), 209–213.
14. Zhang S.T., Tao Z.H., Li W.H., Hou B.R. The Effect of Some Triazole Derivatives as Inhibitors for the Corrosion of Mild Steel in 1M Hydrochloric Acid. *Appl Surf Sci*. 2009, **255**(15), 6757–6783.
15. Azhar M.E., Traisnel M., Mernari B., Gengembrec L., Bentiss F., Lagrene M. Electrochemical and XPS Studies of 2,5-bis(*n*-pyridyl)-1,3,4-thiadiazoles Adsorption on Mild Steel in Perchloric Acid Solution. *Appl Surf Sci*. 2002, **185**(3) 197–205.
16. Behpour M., Ghoreishi S.M., Soltani N., Salavati-Niasari M. The Inhibitive Effect of Some Bis-N,S-bidentate Schiff Bases on Corrosion Behavior of 304 Stainless Steel in Hydrochloric Acid Solution. *Corros Sci*. 2009, **51**(5) 1073–1082.
17. Amar H., Benzakour J., Derja A., Villemin D., Moreau B. and Braisaz T. Piperidin-1-yl-phosphonic Acid and (4-phosphono-piperazin-1-yl) Phosphonic Acid: A New Class of Iron Corrosion Inhibitors in Sodium Chloride 3% Media. *Appl Surf Sci*. 2006, **252**(18), 6162–6172.
18. Bouklah M., Hammouti B., Lagrenee M., Bentiss F. Thermodynamic Properties of 2,5-bis(4-methoxyphenyl)-1,3,4-oxadiazole as a Corrosion Inhibitor for Mild Steel in Normal Sulfuric Acid Medium. *Corros Sci*. 2006, **48**(9) 2831–2842.
19. Algaber A.S., El-Nemma E.M., Saleh M.M. Effect of Octylphenol Polyethylene Oxide on the Corrosion Inhibition of Steel in 0.5M H_2SO_4. *Mater Chem Phys*. 2004, **86**(1) 26–32.
20. Ashassi-Sorkhabi H., Shaabani B., Seifzadeh D. Corrosion Inhibition of Mild Steel by Some Schiff Base Compounds in Hydrochloric Acid. *Appl Surf Sci*. 2005, **239**(2) 154–164.
21. Popova A., Sokolova E., Raicheva S., Christov M. AC and DC Study of the Temperature Effect on Mild Steel Corrosion in Acid Media in the Presence of Benzimidazole Derivatives. *Corros Sci*. 2003, **45**(1), 33–58.
22. Popova A., Christov M., Vasilev A. Inhibitive Properties of Quaternary Ammonium Bromides of N-containing Heterocycles on Acid Mild Steel Corrosion. Part I: Gravimetric and Voltammetric Results. *Corros Sci*. 2007, **49**(8), 3276–3289.
23. Khadom A.A., Yaro A.S., Kadum A.H., AlTaie A.S., Musa A.Y. The Effect of Temperature and Acid Concentration on Corrosion of Low Carbon Steel in Hydrochloric Acid Media. *American Journal of Applied Sciences*. 2009, **6**(7), 1403.
24. Noor E.A., Al-Moubaraki A.H. Thermodynamic Study of Metal Corrosion and Inhibitor Adsorption Processes in Mild Steel/1-methyl-4[4′(-X)-styryl Pyridinium Iodides/hydrochloric Acid Systems. *Mater Chem Phys*. 2008, **110**(1), 145–154.
25. Khadom A.A., Yaro A.S. Protection of Low Carbon Steel in Phosphoric Acid by Potassium Iodide. *Protection of Metals and Physical Chemistry of Surfaces*. 2011, **47** (5), 662–669.
26. Darby R. *Chemical Engineering Fluid Mechanics.* 2nd edition. USA: Marcel Dekker, Inc., 2001. 559 p.
27. AbdulBari H.A., Mohd Yunus R.B., Mahmood W.K., Hassan Z.B. *International Journal of Chemical Technology*. 2008, (1) 1–8.
28. Ahmed M.J., Khadom A.A., Kadhum A.H. Optimization Hydrogenation Process of D-glucose to D-sorbitol Over Raney Nickel Catalyst. *European Journal of Scientific Research*. 2009, **30**(2), 294–304.
29. Khadom A.A., Yaro A.S., Kadhum A.H. Corrosion Inhibition by Naphthylamine and Phenylenediamine for the Corrosion of Copper-Nickel Alloy in Hydrochloric Acid. *Journal of the Taiwan Institute of Chemical Engineers*. 2010, **41**(1), 122–125.
30. Yaro A.S., Al-Jendeel H., Khadom A.A. Cathodic Protection System of Copper-Zinc-Saline Water in Presence of Bacteria. *Desalination.* 2011, **270**(1), 193–198.
31. Zhang S.G., Lei W., Xia M.Z., Wang F.Y. QSAR Study on N-containing Corrosion Inhibitors: Quantum Chemical Approach Assisted by Topological Index. *J Mol Struct-THEOCHEM.* 2005, **732**(1) 173–182.
32. Bereket G., Öğretir C., Özşahin Ç. Quantum Chemical Studies on the Inhibition Efficiencies of Some Piperazine Derivatives for the Corrosion of Steel in Acidic Medium. *J Mol Struc-THEOCHEM*. 2003, **663**(1), 39–46.
33. Martinez S., Tagljar I. Correlation between the Molecular Structure and the Corrosion Inhibition Efficiency of Chestnut Tannin in Acidic Solutions. *J Mol Struc-THEOCHEM.* 2003, **640**(1), 167–174.
34. Bereket G., Hur E., Özşahin Ç. Quantum Chemical Studies on Some Imidazole Derivatives as Corrosion

Inhibitors for Iron in Acidic Medium. *J Mol Struc-THEOCHEM*. 2002, **578**(1), 79–88.

35. Ma H., Chen S., Liu Z., Sun Y. Theoretical Elucidation on the Inhibition Mechanism of Pyridine–pyrazole Compound: A Hartree Fock study. *J Mol Struc-THEOCHEM*. 2006, **774**(1) 19–22.
36. Gao G., Liang C. Electrochemical and DFT Studies of β-amino-alcohols as Corrosion Inhibitors for Brass. *Electrochimica Acta*. 2007, **52**(13), 4554–4559.
37. Lebrini M., Lagrenée M., Traisnel M., Gengembre L., Vezin H., Bentiss F. Enhanced Corrosion Resistance of Mild Steel in Normal Sulfuric Acid Medium by 2,5-bis(*n*-thienyl)-1,3,4-thiadiazoles: Electrochemical, X-ray Photoelectron Spectroscopy and Theoretical Studies. *Appl Surf Sci*. 2007, **253**(23) 9267–9276.
38. Khaled K.F. Adsorption and Inhibitive Properties of a New Synthesized Guanidine Derivative on Corrosion of Copper in 0.5M H_2SO_4. *Appl Surf Sci*. 2008, **255**(5), 1811–1818.
39. Gece G. The Use of Quantum Chemical Methods in Corrosion Inhibitor Studies. *Corros Sci.* 2008, **50**(11), 2981–2992.
40. Lukovits I., Ka´lma´n E., Zucchi F. Corrosion Inhibitors–Correlation between Electronic Structure and Efficiency. *Corrosion.* 2001, **57**(1) 3–8.
41. Musa A.Y., Kadhum A.H., Mohamad A., Takriff M.S. Experimental and Theoretical Study on the Inhibition Performance of Triazole Compounds for Mild Steel Corrosion. *Corros Sci.* 2010, 52(10), 3331–3340.
42. Ebenso E.E., Arslan T., Kandemirli F., Love I., Ogretir C., Saracoglu M., Umoren S.A. Theoretical Studies of Some Sulphonamides as Corrosion Inhibitors for Mild Steel in Acidic Medium. *Int J Quantum Chem*. 2010, **110**(3) 2614–2636.
43. Tromans D., Silva J.C. Behavior of Copper in Acidic Sulfate-solution. *Journal of Electrochemical Society*. 1996, **143**(1), 458–464.
44. Zhang D.Q., Gao L.X., Zhou G.D. Inhibition of Copper Corrosion in Aerated Hydrochloric Acid Solution by Heterocyclic Compounds Containing a Mercapto Group. *Corros Sci.* 2004, **46** (12), 3031–3037.
45. Sherif E.M., Park S.M. Effects of 2-amino-5-ethylthio-1,3,4-thiadiazole on Copper Corrosion as a Corrosion Inhibitor in Aerated Acidic Pickling Solutions. *Electrochimica Acta*. 3006, **51**(28), 6556–6562.
46. Kear G., Barker B.D., Walsh F.C. Electrochemical Corrosion of Unalloyed Copper in Chloride Media – a Critical Review. *Corros Sci.* 2004, **46**(1) 109–135.
47. Roberts R.F. X-ray Photoelectron Spectroscopic Characterization of Copper Oxide Surfaces Treated with Benzotriazole. *J Electron Spectrosc*. 1994, **4**(4), 273–291.
48. Allam N.K., Ashour E.A. Promoting Effect of Low Concentration of Benzotriazole on the Corrosion of Cu10Ni Alloy in Sulfide Polluted Salt Water. *Appl Surf Sci*. 2008, **254**(16), 5007–5011.
49. Babic R., Metikos-Hukovic M., Loncar M. Impedance and Photoelectrochemical Study of Surface Layers on Cu and Cu–10Ni in Acetate Solution Containing Benzotriazole. *Electrochimica Acta*. 1999, **44**(14), 2413–2421.
50. Loo B.H., Ibrahim A., Emerson M.T. Analysis of Surface Coverage of Benzotriazole and 6-tolyltriazole Mixtures on Copper Electrodes from Surface-enhanced Raman Spectra. *Chem Phys Lett*. 1998, **287**(3), 449–454.
51. Polo J.L., Pinilla P., Cano E., Bastidas J.M. Trifenylmethane Compounds as Copper Corrosion Inhibitors in Hydrochloric Acid Solution. *Corrosion*. 2003, **59**(5), 414–423.
52. Villamil R.F., Cordeiro G.O., Matos J., Elia E.D., Agodtinho S.M. Effect of Sodium Dodecylsulfate and Benzotriazole on the Interfacial Behavior of Cu/Cu(II), H_2SO_4. *Mat Chem Phys*. 2002, **78**(2), 448–454.
53. Ma H., Chen S., Niu L., Zhao S., Li S., Li D. Inhibition of Copper Corrosion by Several Schiff Bases in Aerated Halide Solutions. *J Appl Electrochem*. 2002, **32**(1), 65–72.
54. Frigani A., Fonsati M., Monticelli C., Brunoro G. Influence of the Alkyl Chain on the Protective Effects of 1,2,3-benzotriazole Towards Copper Corrosion: Part I. Inhibition of the Anodic and Cathodic Reactions. *Corros Sci.* 1999, **41**(6), 1205–1215.
55. Allam N.K., Nazeer A.A., Ashour E.A. A Review of the Effects of Benzotriazole on the Corrosion of Copperand Copper Alloys in Clean and Polluted Environments. *J Appl Electrochem*. 2009, **39**(4), 961–969.
56. Youda R., Nishihara H., Aramaki K. The Active – Passive Transition in Low Alloy Steels in Carbonate Solutions. *Electrochimica Acta*. 1990, **35**(1), 35–45.

Received 07.02.13
Accepted 10.09.13

Реферат

Объектом исследования была коррозия медно-никелевого сплава, погруженного в соляную кислоту, при разных температурах, концентрациях бензотриазола и скоростях коррозии. Для оценки скорости коррозии использовался метод определения потерь в массе. Полученные результаты показали двойной эффект применения бензотриазола: уменьшилась как коррозия сплава, так и потери в потоке соляной кислоты. Максимальная эффективность ингибирования составила 91,5%, а максимальное уменьшение наволакивания меди было равно 52,4%. Предложен ряд уравнений, описывающих полученные экспериментальные данные с высоким коэффициентом соответствия. Динамическое молекулярное моделирование было применено при исследовании режима адсорбции ингибитора на поверхности медного сплава. Новым в данной работе является проведение аналогии между процессом коррозии и поведением потока соляной кислоты, а также исследование двойного эффекта применения бензотриазола: как ингибитора коррозии и добавки, способствующей уменьшению потерь соляной кислоты.

Ключевые слова: поток жидкости, потери в массе, вращающийся дисковой электрод, кислотная коррозия, уменьшение наволакивания меди.